ESI for: Experimental observations of fractal landscape dynamics in a dense emulsion

Clary Rodríguez-Cruz[a], Mehdi Molaei[a], Amruthesh Thirumalaiswamy[a], Klebert Feitosa[b], Vinothan N. Manoharan[c,d], Shankar Sivarajan[e], Daniel H. Reich[e], Robert A. Riggleman[a‡] and John C. Crocker [a‡*]

S1 Dynamical Scaling State

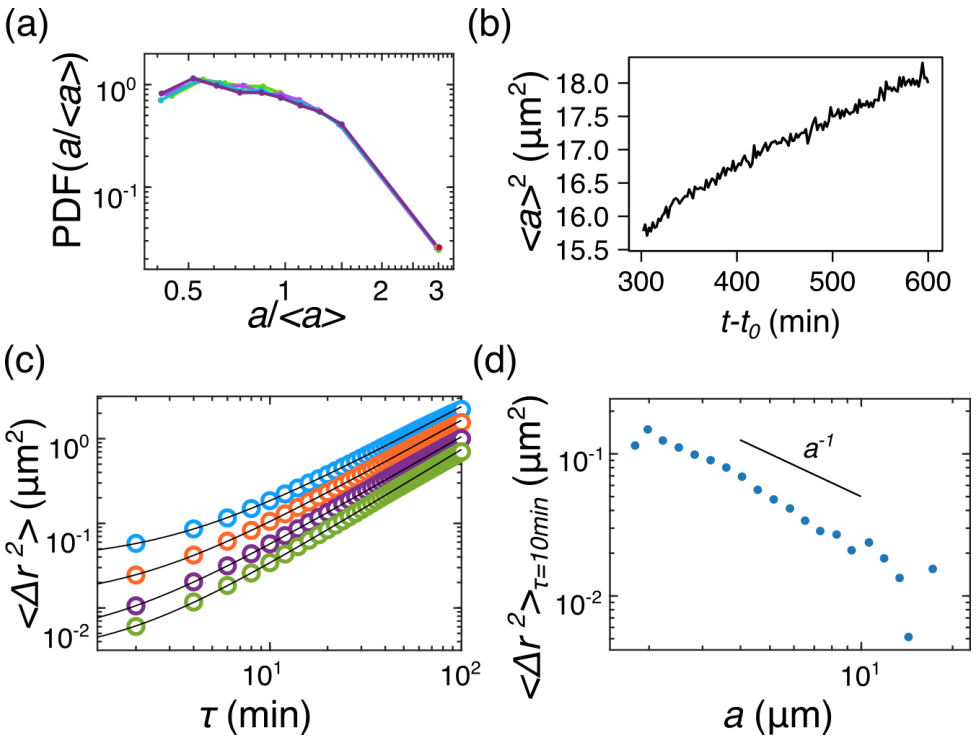

Fig. S1 Experimental system agrees with expected dynamical scaling behavior and polydispersity effects. (a) Droplet size distribution evolution throughout the dynamical scaling period, normalized by the average droplet size, where $t - t_0$ represents time from the beginning of data collection and $t_0 = 7$ hrs is the time from emulsification. (b) Time evolution of the squared average droplet radius shows expected linear relationship. (c) Mean squared displacement of droplet ensembles grouped by radii: [1.60-2.65] μm (blue), (2.65-3.79] μm (orange), (3.79-5.33] μm (purple), (5.33-18.21] μm (green). Black curves show fits to a power law plus a constant $y = ax^b + c$, where $c = 2\sigma^2$ and σ represents measurement error. The displacements of smaller droplets contain larger error, as expected, due to image resolution limitations. (d) Mean squared displacement at $\tau = 10$ min as a function of droplet radius follows the expected a^{-1} behavior.

Figure S1 confirms that the system has reached a dynamical scaling state, where the squared droplet size increases linearly with time and the shape of the size distribution does not change significantly (Figs. S1a,b). As expected for droplets in a mechanical continuum, larger droplets diffuse more slowly (Figs. S1c,d), showing the same scaling as the Stokes-Einstein relation despite being driven by active stress fluctuations.

[a] *Department of Chemical and Biomolecular Engineering, University of Pennsylvania, Philadelphia, PA, USA.*
[b] *Department of Physics and Astronomy, James Madison University, Harrisonburg, Virginia*
[c] *Harvard John A. Paulson School of Engineering and Applied Sciences, Harvard University, Cambridge, Massachusetts*
[d] *Department of Physics, Harvard University, Cambridge, Massachusetts*
[e] *Department of Physics and Astronomy, Johns Hopkins University, Baltimore, Maryland*
‡ These authors contributed equally to this work
* Author to whom any correspondence must be addressed, E-mail: jcrocker@seas.upenn.edu

S2 High-Dimensional Measurement Error Correction

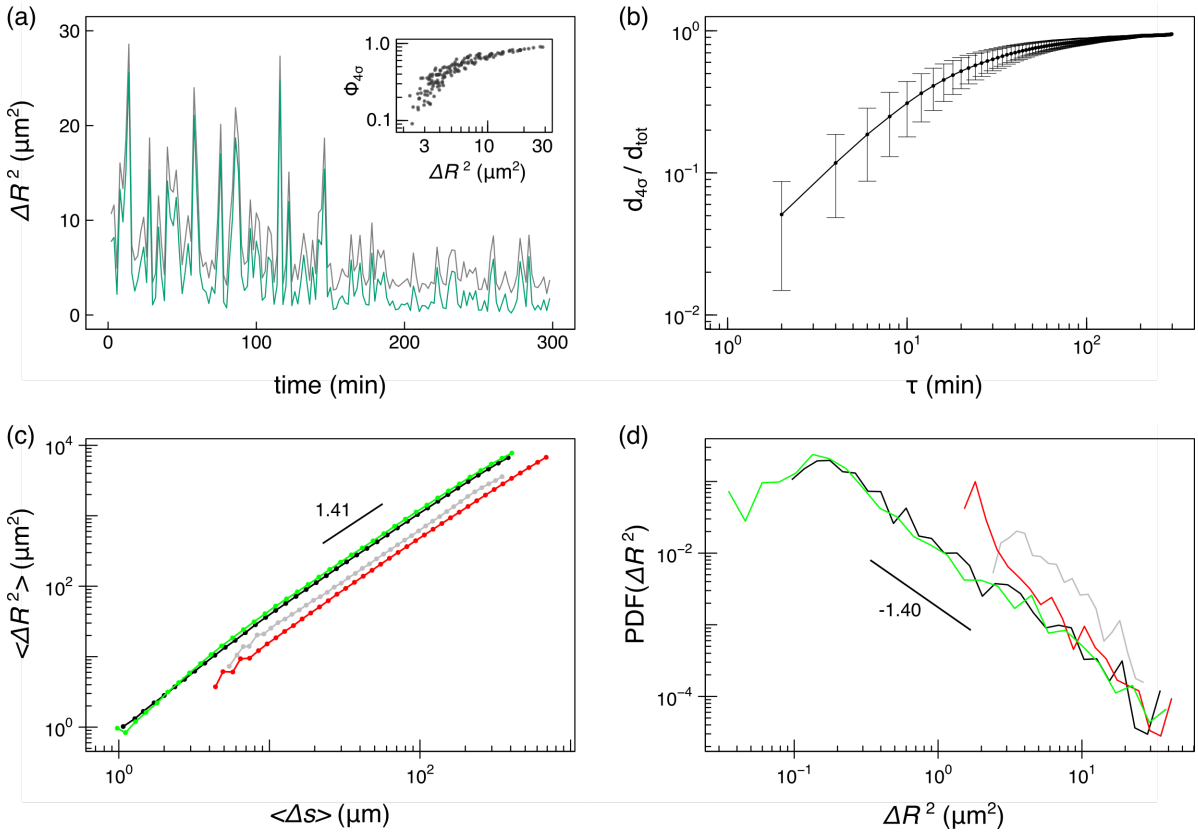

Fig. S2 Gaussian noise effects on high-dimensional displacements. (a) Experimental ΔR^2 before (grey) and after (green) removing measurement error. Inset shows the fraction of droplets moving $> 4\sigma$ for each ΔR^2 value. (b) Fraction of droplets moving $> 4\sigma$ for all τ values. (c) ΔR^2 and Δs between pairs of simulation configurations (black), simulation after adding Gaussian noise (red), and simulation with Gaussian noise after using the noise removal method described in the text (green). Experiment results before removing measurement error are shown in grey. (d) Probability distribution of ΔR^2 for $\tau = 1$ simulation time step and $\tau = 2$ min in the experiment. Color scheme is the same as (c).

The experimental measurement error can be quantified by fitting the mean-squared displacement of individual droplets to a power law plus a constant, $MSD_{xy} = A\tau^B + C$, where $C = 4\sigma^2$. The fit is shown in Fig. 2a (main text), where $4\sigma^2 = 0.0036\ \mu\text{m}^2$ and $\sigma = 0.03\ \mu\text{m}$. This presumably perturbs high-dimensional displacement calculations, especially for low values of τ. To show how random error affects our data, we added a Gaussian-distributed noise signal with zero mean and $\sigma = 0.03\ \mu\text{m}$ to the noise-free simulation data (re-scaled for comparison to the experiment). As shown in Figs. S2c-d (red data), Gaussian error significantly alters the original simulation results by omitting the smallest displacements.

To reduce the sensitivity of our experimental analysis to measurement error, we modified the calculation of all high-dimensional Euclidean distances to exclude any contribution from components/dimensions that were below a threshold. We found empirically that a threshold of 4σ was optimal for the analysis of noisy data to nearly revert to that of the original noiseless data, see Figs. S2c-d (green data). For the distribution of ΔR^2 at $\tau = 1$ simulation time step, noise completely changes the shape and slope of the distribution. This modified calculation was therefore applied to the experimental ΔR^2 and Δs values throughout our analyses in order to reduce systematic errors due to noise in the results. Fig. S2a shows the result of this error correction on the experimental ΔR^2, bringing the noise floor closer to zero, while the inset shows that only a very small fraction of droplets moves $> 4\sigma$ at the smallest ΔR^2 values. This confirms that the smallest ΔR^2 values are most affected by noise, compared to larger values which are dominated by large droplet displacements. Moreover, data at shorter τ values is also more severely affected by noise as shown in Fig. S2b, where the fraction of droplets moving $> 4\sigma$ approaches 1 at large τ.

S3 Emulsion Simulation Displacements

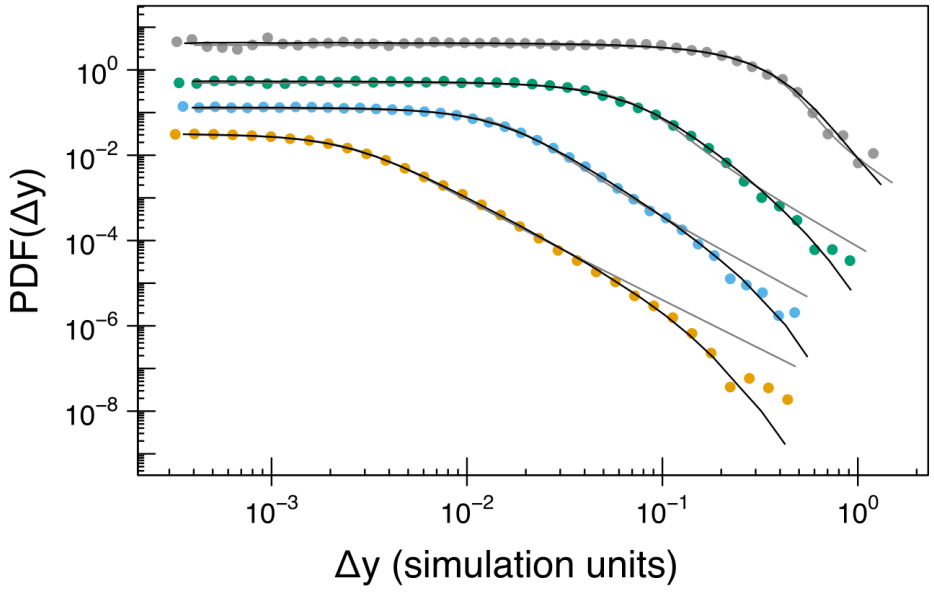

Fig. S3 Van Hove function of simulation droplet displacements for τ = 1, 5, 24, and 140 simulation time units (bottom to top). Solid black curves represent the best fit ETSD and grey curves show the best fit SD.

Figure S3 shows the distribution of droplet displacements in simulations, for multiple values of τ. These are well fit by an ETSD, and the α values from the fits follow a time-varying trend similar to the experimental data (see Fig. S4).

S4 ETSD Shape Parameter

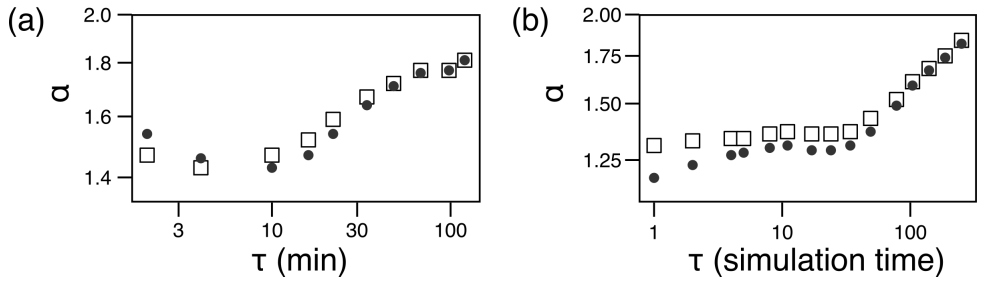

Fig. S4 ETSD stability parameter for the lag-time dependent van Hove displacement distribution, α_{vH} (circles), and for the high-dimensional displacement vector components distribution, α_U (squares), shown for the emulsion experiment (a), and emulsion simulation (b).

We have found that an exponentially truncated stable distribution (ETSD) provides a useful fitting form for the van Hove distribution in systems with fractal landscape dynamics, as shown in Figs. 3 and S3. The stability parameter α from those fits provides a measure of how heavy-tailed the distribution is, related to the exponent of the power-law tail in the untruncated SD. These α values, α_{vH}, show a non-trivial τ dependence shown in Fig. S4, closely resembling that of the high-dimensional displacement vector components, α_U. Both experiment and simulation appear to be trending to a Gaussian value $\alpha = 2$ at long times, due to regression according to the Central Limit Theorem. The near constant value of α_U in the simulation case for small and intermediate lag times confirms the self-similarity of the non-random path directions in configuration space.

S5 Avalanche Clusters

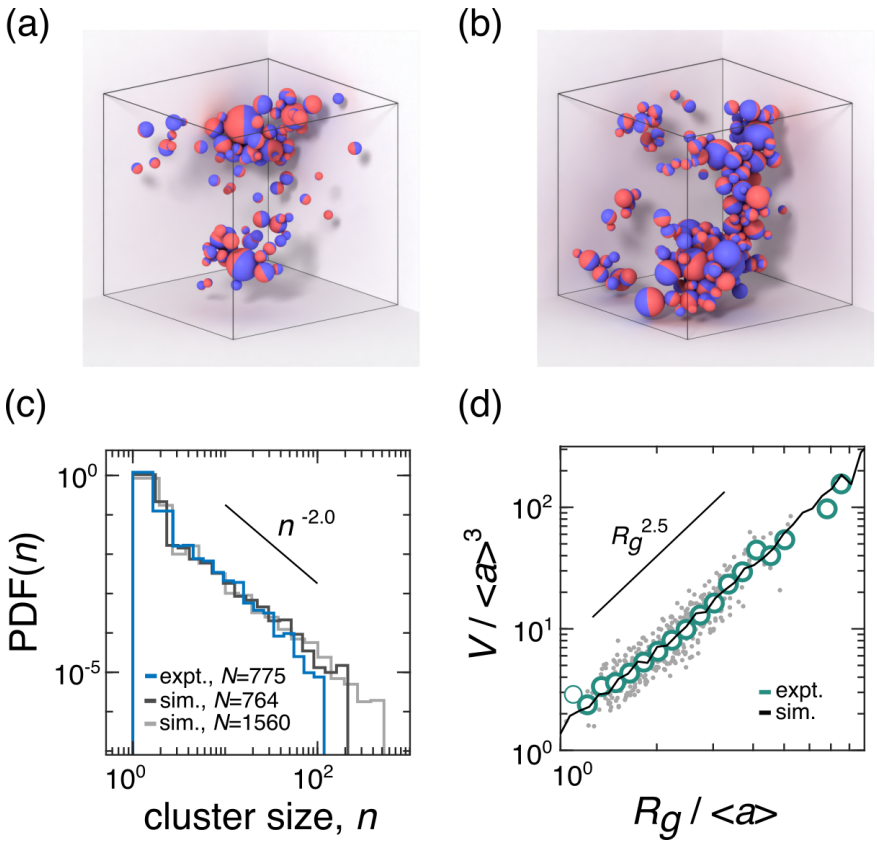

Fig. S5 Cluster analysis for droplets with the largest displacements. (a,b) Simulation data renders of the particles moving in the top 5% of all particles at 2 different time points, calculated with the same experimental threshold method described in the text. (c) Distribution of the number of droplets, n, in each cluster shows power law scaling for both experiment and simulation. (d) The volume of individual clusters, V, shows a power law dependence on their radius of gyration, R_g, confirming their fractal shape and matching the averaged simulation results (line). Green circles are averages of the grey data points.

The droplets with the largest displacements between consecutive confocal images ($\tau = 2$ min) were determined by using a time-dependent threshold, constructed so that 5% of droplets were above threshold on a time averaged basis. These particles were formed into clusters using an adjacency matrix that specifies which droplets are contacting neighbours. Droplets were considered to be in contact if their center-to-center separation was less than 1.1 times the sum of their radii, to allow for measurement error and droplet distortion. Our findings were not sensitive to this factor. The resulting clusters from the experiment show fractal scaling (Figs. S5c-d) and are similar to those observed in the simulations (Figs. S5a-b).

Notes and references

1 J. Renn, *Annalen der Physik*, 2005, **14**, 23–37.
2 H. G. Schuster and W. Just, *Deterministic chaos: an introduction*, John Wiley & Sons, 2006.
3 V. Zaburdaev, S. Denisov and J. Klafter, *Reviews of Modern Physics*, 2015, **87**, 483.
4 A. Gopal and D. J. Durian, *Physical Review Letters*, 1995, **75**, 2610.
5 P. Hébraud and F. Lequeux, *Physical Review Letters*, 1998, **81**, 2934.
6 P. Sollich, F. Lequeux, P. Hébraud and M. E. Cates, *Physical Review Letters*, 1997, **78**, 2020.
7 B. Fabry, G. N. Maksym, J. P. Butler, M. Glogauer, D. Navajas and J. J. Fredberg, *Physical Review letters*, 2001, **87**, 148102.
8 B. D. Hoffman and J. C. Crocker, *Annual Review of Biomedical Engineering*, 2009, **11**, 259–288.
9 E. I. Corwin, H. M. Jaeger and S. R. Nagel, *Nature*, 2005, **435**, 1075–1078.
10 M. van Hecke, *Journal of Physics: Condensed Matter*, 2009, **22**, 033101.
11 P. K. Morse and E. I. Corwin, *Physical Review Letters*, 2017, **119**, 118003.
12 V. V. Vasisht, S. K. Dutta, E. Del Gado and D. L. Blair, *Physical Review Letters*, 2018, **120**, 018001.
13 F. Giavazzi, V. Trappe and R. Cerbino, *Journal of Physics: Condensed Matter*, 2020, **33**, 024002.
14 J. Song, Q. Zhang, F. de Quesada, M. H. Rizvi, J. B. Tracy, J. Ilavsky, S. Narayanan, E. Del Gado, R. L. Leheny, N. Holten-Andersen *et al.*, *Proceedings of the National Academy of Sciences*, 2022, **119**, e2201566119.
15 H. J. Hwang, R. A. Riggleman and J. C. Crocker, *Nature Materials*, 2016, **15**, 1031–1036.
16 D. J. Wales, J. P. K. Doye, M. A. Miller, P. N. Mortenson and T. R. Walsh, *Energy Landscapes: From Clusters to Biomolecules*, John Wiley & Sons, Ltd, 2007, vol. 115, pp. 1–111.
17 G. Lois, J. Blawzdziewicz and C. S. O'Hern, *Physical Review E*, 2010, **81**, 051907.
18 P. Charbonneau, J. Kurchan, G. Parisi, P. Urbani and F. Zamponi, *Nature Communications*, 2014, **5**, 1–6.
19 J. Clara-Rahola, T. Brzinski, D. Semwogerere, K. Feitosa, J. Crocker, J. Sato, V. Breedveld and E. R. Weeks, *Physical Review E*, 2015, **91**, 010301.
20 R. Penfold, A. D. Watson, A. R. Mackie and D. J. Hibberd, *Langmuir*, 2006, **22**, 2005–2015.
21 T. Savin and P. S. Doyle, *Biophysical Journal*, 2005, **88**, 623–638.
22 D. S. Martin, M. B. Forstner and J. A. Käs, *Biophysical Journal*, 2002, **83**, 2109–2117.
23 P. Stevenson, *Current Opinion in Colloid & Interface Science*, 2010, **15**, 374–381.
24 K. Feitosa, O. L. Halt, R. D. Kamien and D. J. Durian, *EPL (Europhysics Letters)*, 2006, **76**, 683.
25 D. J. Durian, *Physical Review Letters*, 1995, **75**, 4780.
26 S. Tewari, D. Schiemann, D. J. Durian, C. M. Knobler, S. A. Langer and A. J. Liu, *Physical Review E*, 1999, **60**, 4385.
27 I. K. Ono, S. Tewari, S. A. Langer and A. J. Liu, *Physical Review E*, 2003, **67**, 061503.
28 T. Solomon, E. R. Weeks and H. L. Swinney, *Physical Review Letters*, 1993, **71**, 3975.
29 E. R. Weeks and H. L. Swinney, *Physical Review E*, 1998, **57**, 4915.
30 B. B. Mandelbrot and J. W. Van Ness, *SIAM Review*, 1968, **10**, 422–437.
31 A. W. Lau, B. D. Hoffman, A. Davies, J. C. Crocker and T. C. Lubensky, *Physical Review Letters*, 2003, **91**, 198101.
32 P. Grassberger and I. Procaccia, *Physical Review Letters*, 1983, **50**, 346–349.
33 F. A. Lavergne, P. Sollich and V. Trappe, *The Journal of Chemical Physics*, 2022, **156**, 154901.
34 R. N. Mantegna and H. E. Stanley, *Physical Review Letters*, 1994, **73**, 2946.
35 L. Cipelletti, L. Ramos, S. Manley, E. Pitard, D. A. Weitz, E. E. Pashkovski and M. Johansson, *Faraday Discussions*, 2003, **123**, 237–251.
36 D. W. Swartz and B. A. Camley, *Soft Matter*, 2021, **17**, 9876–9892.
37 S. Stoev and M. S. Taqqu, *Fractals*, 2004, **12**, 95–121.
38 K. Burnecki and A. Weron, *Physical Review E*, 2010, **82**, 021130.
39 E. R. Weeks, J. C. Crocker, A. C. Levitt, A. Schofield and D. A. Weitz, *Science*, 2000, **287**, 627–631.
40 C. P. Massen and J. P. Doye, *Physical Review E*, 2007, **75**, 037101.
41 H. Yoshino and F. Zamponi, *Physical Review E*, 2014, **90**, 022302.
42 C. Rainone, P. Urbani, H. Yoshino and F. Zamponi, *Physical Review Letters*, 2015, **114**, 015701.
43 G. Biroli and P. Urbani, *Nature Physics*, 2016, **12**, 1130–1133.
44 P. Charbonneau, J. Kurchan, G. Parisi, P. Urbani and F. Zamponi, *Annual Review of Condensed Matter Physics*, 2017, **8**, 265–288.
45 M. Baity-Jesi, L. Sagun, M. Geiger, S. Spigler, G. B. Arous, C. Cammarota, Y. LeCun, M. Wyart and G. Biroli, International Conference on Machine Learning, 2018, pp. 314–323.

46 G. Chen, C. K. Qu and P. Gong, *Neural Networks*, 2022, **149**, 18–28.
47 Y. Shi, C. L. Porter, J. C. Crocker and D. H. Reich, *Proceedings of the National Academy of Sciences*, 2019, **116**, 13839–13846.
48 Y. Shi, S. Sivarajan, K. M. Xiang, G. M. Kostecki, L. Tung, J. C. Crocker and D. H. Reich, *Integrative Biology*, 2021, **13**, 246–257.
49 Y. LeCun, Y. Bengio and G. Hinton, *Nature*, 2015, **521**, 436–444.